Measurement of Forces in Symmetric and Asymmetric Interactions between Diblock Copolymer Layers Adsorbed on Mica

Hiroshi Watanabe

Department of Macromolecular Science, Faculty of Science, Osaka University, Toyonaka, Osaka 560, Japan

Matthew Tirrell*

Department of Chemical Engineering and Materials Science, University of Minnesota, Minneapolis, Minnesota 55455

Received May 19, 1993; Revised Manuscript Received September 7, 1993®

ABSTRACT: Measurements have been made of the forces of interaction between pairs of layers of diblock copolymers adsorbed on mica from toluene in a surface forces apparatus. The copolymers studied were poly(2-vinylpyridine)–polyisoprene (PVP–PI) and poly(2-vinylpyridine)–polystyrene (PVP–PS), over a range of molecular weights of each of the blocks. Previous studies of adsorption of similar polymers under similar conditions have shown that the PVP blocks ("anchors") preferentially adsorb and anchor the PS and PI blocks ("buoys") effectively by their ends at a density high enough to cause substantial overlap among the buoys. The ranges of the forces measured in this study are consistent with previous observations that this overlap causes the PS or PI chains to be tethered to the anchor layer in a configuration that is extended in the direction normal to the surface relative to the dimensions of a free chain of equal molecular weight in toluene solution, thereby creating a polymer "brush". All of the force versus distance data on six pairs of symmetrical interactions between these layers collapse with reasonable accuracy in a reduced plot, the variables of which are suggested by models of the interactions between grafted layers developed by Patel et al. and by Milner et al. The shape of this universal profile is predicted well by both models, with a small advantage to the latter. There are no free parameters in this comparison; the necessary data on solvent quality, segment size, and number density of chains on the surface were determined independently. Both models underpredict the force and its range by a factor of about 2 when the osmotic pressure data for homopolymer solutions are used in the calculation, while good agreements are found when the osmotic pressure is determined from the surface force data at high compression. Measurements have also been made of three distinct situations of asymmetric interaction between dissimilar layers. These asymmetries are *chemical*, between a PS layer and a PI layer at equal surface density and equal brush height, *molecular weight*, between two different PS brushes that have equal surface number density of chains but different chain lengths, and *structural*, between two different PI layers that have different molecular weights and surface number densities but about the same weight per unit area of polymer brush chain bound to the surface. The first two cases give results that are readily anticipated from the knowledge of the behavior of symmetrical interactions between brushes which shows that there is little interpenetration between two equally dense brushes. Structural asymmetry appears to give rise to more substantial interpenetration, or rearrangement, producing forces of a magnitude that are somewhat smaller than those anticipated from the noninterpenetration idea. Pull-off forces were also measured between thoroughly dried layers of the PS- and PI-containing copolymers. These data are converted into adhesive energies and compared with literature values for surface energies of bulk PS and PI.

Introduction

The adsorption behavior of copolymers is naturally richer than that of polymers containing only a single kind of segment since more than one kind of affinity can be built into different parts of the same macromolecule. The interfacial activity of such polymers can be enhanced and manipulated by incorporating segments tailored to interact in some specific way with each of the contacting phases. Architecture of the copolymer plays an important role since it influences the configuration adopted by the molecule at the interface.

Among many interesting and useful possibilities, selective adsorption of block copolymers from selective solvents merits study since it is one means of binding a polymer chain to a surface on which it would not itself adsorb. This can be used to modify the surface of a solid and thereby to manipulate the interactions that this surface experiences. In the case of diblock copolymers, this mode of adsorption is one means of creating a polymer "brush", where polymer chains are tethered by their ends onto an interface.[1,2] The adsorbing block serves as the "anchor" and the tethered chain as the "buoy".[3] A brush results when the density of adsorption is sufficiently high that the buoy chains begin to overlap substantially and stretch normal to the surface to alleviate the buildup of osmotic pressure in the dense brush. Alexander[4] and de Gennes[5] first analyzed this situation and showed that the stretching of the brush would be balanced by the stretching energy built into the chain. Subsequent analyses have developed these ideas more fully.[6–9]

Two lines are pursued in this research. One is the study of the process of selective adsorption of block copolymers from selective solvents as a means of creating polymer brushes. There is incomplete understanding of the factors that determine the assembly of these layers and how the nonadsorbing buoys arrange themselves within the brush. We present an ensemble of data here on six copolymers, varying the chemical type of the nonadsorbing blocks and the molecular weights of each block, where both the adsorbed amount of the block copolymers and some measure of the profile of segments extending into solution have been determined precisely on the identical adsorbed

® Abstract published in *Advance ACS Abstracts*, October 15, 1993.

0024-9297/93/2226-6455$04.00/0

layers. We report data here using the surface forces apparatus[10] in which both the quantity and the profile of segments have been studied by compressing the adsorbed layers and measuring the force versus distance profile between them. The force profile for the layer immersed in solvent is directly related to the segment distribution for which several predictions[6-9] have been made concerning its shape. The quantities of polymer adsorbed in each case can be measured on the same layers with the solvent having been thoroughly evaporated. The determination proceeds from the direct physical measurement of the thicknesses of the layers and the known densities and compositions of the materials involved. This enables a comparison to be made between models of the profiles and the data with no adjustable parameters. In particular, we attempt to assess quantitatively through these data the degree to which the predicted parabolic nature of the segment distribution[6] affects the observable force profile.

A second line of research that is opened up in this work is the manipulation of the interactions between polymer brushes by controlled variations in the construction of the brushes. Many interesting variations are conceivable. Dense polymer brushes contain stretched chains which possess several interesting characteristics. One of these characteristics is that, with increasing stretching (produced by increasing density of chains), there is an increasing tendency for chain ends to populate preferentially the tip region of the brush. One could imagine this as a means to drive a particularly selected chemical functionality to the periphery of the brush. A second important characteristic is the resistance of dense polymer brushes to penetration by extrinsic polymer segments.[11] This arises from the stretched condition of the brush and the resultant strong penalty that would be incurred by the further stretching necessary to swell and accommodate additional segments entering the brush.

Specifically, we present data on asymmetric interactions between dissimilar polymer brushes. We show how pairs consisting of two different brushes can be assembled in a configuration suitable for force measurement and study the interactions that develop on compression. These data are valuable directly for their applicability to practical examples of asymmetric interaction[12] and also indirectly for the information they provide on the mutual interpenetrability of dense polymer brushes.

We study poly(2-vinylpyridine)–polyisoprene (PVP–PI) in addition to the poly(2-vinylpyridine)–polystyrene (PVP–PS) polymers we have studied previously.[13] Two reasons for this are as follows: (a) we surmised that, being a room temperature rubber, the PI block might form a more uniform layer in the dry state and therefore be more amenable to the direct mechanical squeezing determination of the adsorbed amount, a method we introduce in this paper (this proved unfounded; the PVP–PS polymers were equally suitable), and (b) availability of the PI blocks enabled the study of the chemically asymmetric interaction between a PS and a PI brush.

Experimental Section

Material Synthesis. Four PVP–PI diblock copolymers were synthesized by anionic polymerization techniques in high vacuum. The monomers (isoprene, 2-vinylpyridine), polymerization solvent (*n*-heptane, tetrahydrofuran), and terminator (methanol) were purified by standard methods.[14-16] The initiator (*sec*-butyllithium) was synthesized from lithium metal and *sec*-butyl bromide.[14]

The PI blocks were synthesized in *n*-heptane via the two-step reaction suggested by Fujimoto,[14] which produces a narrow molecular weight distribution. First, a small fraction of a prescribed amount of the isoprene monomer was initiated by *sec*-butyllithium at 60–65 °C for 20 min, so that all *sec*-butyllithium molecules are converted into isoprenyl anions and lithium cations. Then, the remaining (major) part of the isoprene monomer was introduced in the reaction flask and allowed to polymerize at room temperature for 48 h. The PI concentration in the flask was typically 2 wt %. The PI blocks made by this method have a typical microstructure cis:trans:vinyl = 75:20:5.[17]

Table I. Characterization of PVP–PI Block Copolymers

code	PVP–PI copolymer			precursor PI	
	$10^{-3}M^a$	ϕ_{PVP} (wt %)[b]	M_w/M_n	$10^{-3}M_w$	M_w/M_n
PVP–PI 26–50	76.6	34.2	1.12	50.4	1.07
PVP–PI 30–217	247	12.3	1.18	217	1.11
PVP–PI 38–69	107	35.2	1.14	69.3	1.08
PVP–PI 69–39	108	64.1	1.16	38.8	1.07

[a] $M^{PVP-PI} = M_w^{PI}/(1 - \phi_{PVP})$. [b] PVP content determined by UV and refractive index monitors in GPC.

After the polymerization of PI blocks, an aliquot (the precursor for copolymer samples) was taken for the later characterization. Most (>90%) of the *n*-heptane was then removed from the reaction flask, and nearly the same amount of tetrahydrofuran was introduced. Both transfers were made by vacuum distillation. The 2-vinylpyridine monomer was copolymerized with living PI blocks in this mixed solvent (with much excess of tetrahydrofuran) at −78 °C. After 2 h of polymerization, the reaction was terminated with methanol. After the reaction, the entire contents of the reaction flask were poured into a 1/2 methanol/water mixture to recover the PVP–PI block copolymer. The copolymer was dried in vacuum and redissolved in benzene, the solution was filtered, and the copolymer finally freeze-dried and stored in vacuum until use.

The copolymer samples were characterized with respect to molecular weight and copolymer composition using a gel permeation chromatograph (GPC; Waters, Model 150-C) with a UV monitor (ABI Analytical Kratos Division, Spectroflow 757) connected in series to a built-in refractometer. The elution solvent was tetrahydrofuran, and monodisperse homopolyisoprenes made and characterized by light scattering at Osaka University[18] were used as the elution standards. Table I summarizes the characterization of the PVP–PI samples. The two PVP–PS copolymers used were characterized previously.[13] The code numbers indicate the molecular weights of the blocks in thousands.

Force Measurements. The mica used for the surface force measurements was Grade No. 4 ASTM V-2, clear and slightly stained Muscovite, ruby red mica obtained from Asheville-Schoonmaker Mica Co. The thickness and area of the mica sheets used were 1–3 μm and ≈1 cm², respectively. Force measurements were carried out on the University of Minnesota surface forces apparatus which is very similar to the original Israelachvili design.[19] The basic techniques and standard experimental procedures we employ in making force measurements on block copolymers are described elsewhere.[10,13] We give a few details here. In what follows, by symmetric layers, we mean situations where identical adsorbed layers are assembled on the two surfaces; asymmetric layers refers to the cases where we assemble and measure interactions between two different block copolymer layers, one on each surface.

Symmetric Layers. Surface force measurements were carried out for the PVP–PI copolymers shown in Table I, as well as for two PVP–PS copolymers, 60–60 and 60–90, examined in a previous study.[9,13,20,21] Those copolymers were adsorbed on mica sheets in the surface force apparatus from toluene solutions at concentrations of about 5 μg/mL. Other work from our laboratories[22] has shown that the weight adsorbed per unit area for these copolymers is quite insensitive to solution concentration in this range, though the complete adsorption isotherms over wide ranges of concentration may bear further study. Glass-distilled, spectroscopic grade toluene was used after filtration without further purification.

Within 6 h of adsorption time, the force–distance profiles became constant in time. The forces, F, between the adsorbed layers were measured at 32 °C several times completely inde-

pendently, each time using freshly prepared adsorption solutions and fresh mica surfaces, confirming the reproducibility of the data. In each measurement, several spots on the mica surface were examined, confirming the uniformity of the adsorbed layer. All data are plotted on the basis of the Derjaguin approximation[23] in which the force, $F(D)$, at some distance, D, of closest approach between the curved mica sheets is divided by the radius of curvature, R. This quantity, for $D \ll R$, is 2π times the energy per unit area of interaction at D, a geometry-independent quantity.[24]

After the measurements in the toluene solution, the solution (≈350 mL in volume) was drained and pure toluene was charged in the apparatus. The inside of the apparatus, with the two copolymer layers separated by more than 4 mm, was bathed in pure toluene for more than 4 h. When the solution was drained, the two mica surfaces were brought to a separation of about 1 mm, so that a small volume of solvent was kept in this narrow gap and the adsorbed layers were always wet with toluene. This washing procedure was repeated at least three times. After that, the amount of nonadsorbed copolymer chains remaining in the apparatus was extremely small. (From the concentration of the feed solution and the dilution rate, this amount is estimated to be less than 10^{-11} g, which is much smaller than the amount of the adsorbed copolymers.) The apparatus was refilled with pure toluene, and the force was remeasured. In all cases, the data obtained in pure toluene were the same as those in the solution, suggesting that no significant desorption took place in the time scale of our experiments (≈5 days).

Asymmetric Layers. To obtain surface force data between asymmetric layers, we prepared three or four mica sheets of equal thickness (in the range 1–3 μm). Two of them were used for the surface force measurements for the symmetric layers of the first species, as explained above. The remaining one or two sheets (glued on glass lenses) were used to prepare the adsorbed layers of the second species. The adsorption of this second species was carried out in a separate glass container under conditions similar to those for the experiments for the symmetric layers. After saturation (>6 h), the mica sheets were immersed in pure toluene (solvent) three or four times to remove all nonadsorbed chains and were stored in pure toluene until use. (Those adsorbed layers were prepared just before use to avoid possible contamination and were never stored in toluene for a period of time longer than 4 h.)

After completion of the symmetric surface force measurements for the two layers of the first species in pure toluene, the upper layer (fixed in an interchangeable holder) was quickly replaced by the layer of the second species previously prepared as described above. The surface force measurements were then made for the resulting assembly of the asymmetric layers, with the upper and lower layers being composed of the second and first species, respectively. In cases where there was a fourth mica sheet carrying the layer of the second species, we also subsequently exchanged the lower layer, mounted on the leaf spring in the surface force apparatus, to make measurements on the symmetric pair of the layers of the second species as a control. The data obtained were compared with the data obtained for those symmetric layers prepared directly in the surface force apparatus. All data reported here are on systems where this second, control, symmetric experiment gave results identical to the directly prepared symmetric layers.

Measurements on Dry Layers To Determine Surface Coverage and Adhesive Energy. On completion of each independent force measurement in pure toluene for symmetric layers, the toluene was drained and the adsorbed layers of copolymers were dried, unless the successive measurements on asymmetric layers were planned. The two adsorbed layers were separated by more than 4 mm and dried in the apparatus by passing clean nitrogen gas through the apparatus for more than 12 h. The two layers were then brought toward contact.

For PVP–PI layers, where the rubbery PI blocks form the top surface in the dry state, the two layers achieved spontaneous, flat, adhesive contact by jumping together, as observed by the sudden flattening of the shapes of the interference fringes when the two surfaces were brought to within separations over which molecular forces could act.[25] The sharp corners in the shapes of the fringes when contact occurred suggest that the contact is attractive.[26] The size of the flat portion of the fringes can be measured and converted into the area of adhesive contact between the two surfaces. On application of compressive load, there was no variation in the fringe positions, but the area of contact increased. This also suggests that molecular adhesive contact was obtained.

Table II. Characteristics of Block Copolymer Layers

copolymer		$2L_{contact}$ (Å)[a]	$10^{-16}\sigma$ (m^{-2})	$10^{-16}\sigma^*$ (m^{-2})[b]
PVP–PI	26–50	33	1.25	0.39
	30–217	30	0.34	0.067
	38–69	37	1.00	0.26
	69–39	31	0.87	0.52
PVP–PS	60–60[c]	31	0.82	0.48
	60–90[d]	43	0.88	0.28

[a] $2L_{contact} = D$ measured at molecular contact of dry layers. [b] $\sigma^* = 1/\pi\langle s^2\rangle$. [c] $10^{-3}M_{PVP} = 60$, $10^{-3}M_{PS} = 60$. [d] $10^{-3}M_{PVP} = 60$, $10^{-3}M_{PS} = 95$.

Under these circumstances, the combined thickness of the two layers in contact was evaluated from the positions of the observed interference fringes. The number of copolymer chains per unit area (σ) was then calculated from the known molecular weights and bulk densities of the constituent blocks.

For PVP–PS layers, the situation was somewhat different. On close approach of the two dry layers, where the glassy PS blocks form the top surface (this arrangement has been experimentally confirmed in previously published work[22]), the first contact (determined from the cessation of vibrations of the fringes) was not adhesive. Application of compressive load on the contact caused the two surfaces to move closer together, as seen by the shifting wavelengths of the interference fringes. This was accompanied by an eventual flattening of the surfaces into a molecular, adhesive contact, with characteristics as observed for the PVP–PI layers. If the surfaces are separated from this initial molecular contact, then brought back toward contact a second time at the same spot, they jump spontaneously into flat, adhesive contact. The observations suggest that the glassy layers are not smooth in the as-dried state; however, they are readily compressed into adhesive, molecular contact. In this state, σ was determined as described above. In measurements on identical polymers, the data on σ reported here agree within experimental error (≈±10%) with values we have previously reported,[22] obtained by radio-labeling and X-ray photoelectron spectroscopy. The data on the adsorbed amounts of all the copolymers studied here are given in Table II.

We also measured the adhesive force exerted between the dried, symmetric layers. By applying a tensile force to the two surfaces in adhesive contact, they could be made to jump apart by the action of the leaf spring on which the lower surface sites.[25,27] Measurement of the distance of the jump and of the stiffness of the spring gives the adhesive force by a standard calculation. We report these data here as interfacial energies, calculated from the JKR theory of adhesive contact mechanics.[26] Previous work from other laboratories[25] and ours[27] argues for the validity of this model. The shapes of the interference fringes we observed here, and the fact that the two surfaces appeared to jump apart from a finite radius of contact, further support the JKR theory as the means to calculate interfacial energy from pull-off force. Pull-off forces could be measured repeatedly and reproducibly from the same contact spot, indicating that the adhesive force measurement did not damage the surfaces.

Results and Discussion

Force–Distance Profiles for Symmetric Layers. Figure 1 shows the dependence of the forces on distance between the mica substrates for the six polymers for which the molecular and adsorption characteristics are given in Tables I and II. All of the block copolymers, in good solvent conditions for the nonadsorbing blocks, exhibit monotonic repulsion, as has been reported previously.[13] Detectable repulsion is seen for all of the polymers at a range which exceeds (by more than a factor of 10 in some cases) the dimension in free solution of the nonadsorbing blocks of

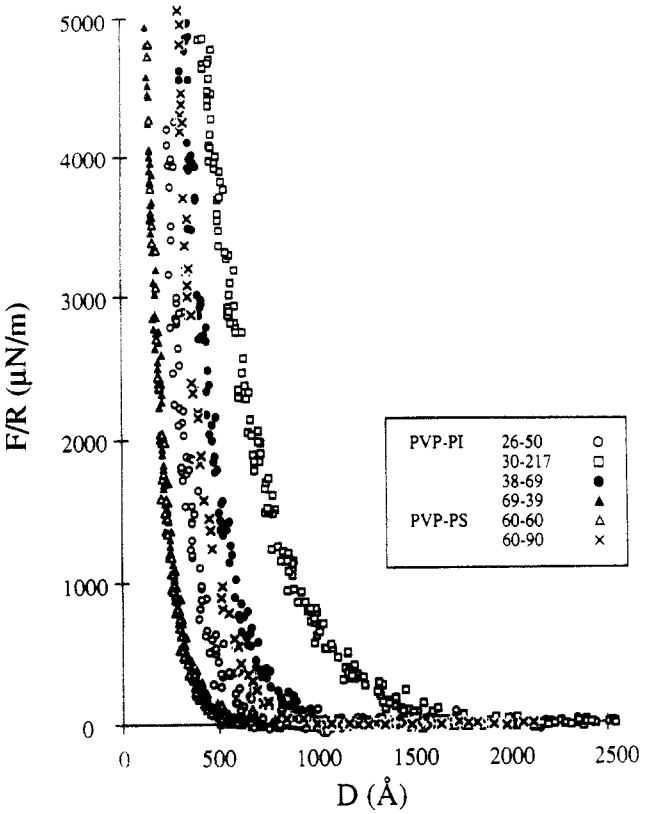

Figure 1. Force–distance profiles obtained for the PVP–PI and PVP–PS block copolymer layers in toluene at 32 °C.

comparable molecular weights. Table II documents that all of these copolymers adsorb on the surface at an average distance between chains which is less than the average dimension of the same molecule in solution. The surface number density of chains exceeds (by a factor of 1.5–5) the density required for mutual overlap, creating a semidilute surface layer or polymer brush.[3] Previous work[22] has established that chains of this type adsorb through the PVP block and that both blocks play a role in dictating the final adsorbed amount.

Comparison with Bulk Osmotic Pressure Data. With the interaction curves and adsorbed amounts determined experimentally, we can attempt to determine the relationship among the force curves measured for different molecular weights and surface densities. For that purpose, it is necessary that the other important parameters governing the behavior of the system be known. The necessary additional parameters are those that determine the configurational properties of the polymers and those that fix the osmotic pressure for a certain monomer segment density in solution.

Configurational properties of interest are those related to the dependence of radius of gyration on chain length. For monodisperse PI and PS in toluene, the molecular weight dependencies of the intrinsic viscosities are very similar:[28]

$$[\eta] = 10.5 \times 10^{-3} M^{0.73} \text{ (mL/g) for PS} \qquad (1)$$

$$[\eta] = 20.0 \times 10^{-3} M^{0.728} \text{ (mL/g) for PI} \qquad (2)$$

suggesting that the molecular weight dependence of chain dimensions in solution is almost exactly the same for PS and PI. Employing the Flory–Fox equation,[29] we can estimate the mean-square radius of gyration, $\langle s^2 \rangle$, of PI from that of PS of the same molecular weight by[30]

$$\langle s^2 \rangle^{3/2}_{PI} = \{[\eta]_{PI}/[\eta]_{PS}\}\langle s^2 \rangle^{3/2}_{PS} \qquad (3)$$

The data for $\langle s^2 \rangle_{PS}$ in toluene reported by Higo et al.[31] are summarized as

$$\langle s^2 \rangle^{1/2}_{PS} = b_{PS} N_{PS}^{\nu} \qquad b_{PS} = 1.86 \text{ Å} \qquad \nu = 0.595 \qquad (4)$$

where b_{PS} and N_{PS} represent the segment length and degree of polymerization of PS, respectively. From these relationships, we can estimate $\langle s^2 \rangle^{1/2}_{PI}$ as

$$\langle s^2 \rangle^{1/2}_{PI} = b_{PI} N_{PI}^{\nu} \qquad b_{PS} = 1.79 \text{ Å} \qquad \nu = 0.595 \qquad (5)$$

These formulas are the ones we have used to determine the surface overlap densities reported in Table II, confirming that these adsorbed layers have indeed entered, albeit not in all cases very deeply, into the brush regime.[1,5]

In developing an understanding of the interrelationships among the force curves of Figure 1, we must recognize that two factors contribute to the forces exerted between the two brushes at some separation D.[8,9] One is the osmotic interaction in the PS or PI layer, which generates forces tending to increase the separation in order to dilute the layer with the good solvent toluene; the other is the entropic elasticity of the PS or PI blocks, which tends to decrease the layer thickness from the osmotically swollen thickness. When we *impose* a compression to some value of D in the surface forces apparatus where the two brushes are interacting, we expect that, at high enough compression, the osmotic pressure forces from the two interacting brushes will overwhelm the elastic forces since the confinement resulting from compression will reduce the chain stretching. Thus, for the smallest values of D that we examine, we expect that the forces exerted by these layers will be very similar to that of homopolymer solutions at the same concentrations. This is expected to be true, irrespective of the molecular weights and surface densities of the polymers involved, providing that the comparison among the data on different polymers is scaled to equivalent concentrations of polymer in the gap between the two surfaces.

The osmotic free energy per unit area for the interacting brushes will be determined by the average concentration of chain segments in the gap, c, which is in turn determined by the mass of polymer adsorbed per unit area, w, and the separation between the mica sheets, D. The contention that the osmotic pressure effects dominate other factors at higher compressions means that the force–separation profile should become scaled only in terms of c in that limit. To test this, we evaluate w and c from our data on surface coverage, σ:

$$w = 2\sigma M_B/N_{av} \qquad c = w/(D - 2L_{PVP}^{\circ}) \qquad (6)$$

The average concentration is just the weight per unit area divided by the separation between the surfaces, subtracting off a small correction for the thickness (L_{PVP}°) of the PVP layers on top of which the PI or PS brushes sit. (The subscript B refers to either PS or PI.) L_{PVP}° is determined from $L_{contact}$ in Table II and the bulk densities of the polymers. (In toluene, PVP appears to be swollen by about 50%.[22] However, the factor L_{PVP}° gave only a small correction for $c(D)$ in the range of D examined, so we neglected the PVP swelling effect in calculating the average concentration of segments in the gap.)

These calculations of the average concentration in the gap show that the average concentration varies up to 0.15 g/cm^3 in the range of compressions used in our experiments. Thus, without assuming any molecular model for the

behavior of polymer brushes, we can compare the behavior of these copolymer layers and semidilute homopolymer solutions. Data for osmotic pressure, Π, in PS–toluene solutions in this concentration range have been reported by Noda et al.[32,33] The data are in good agreement with a power-law concentration dependence[34] expressed as

$$\Pi(M_{PS}/N_{av})/ckT = K_{\Pi}(c/c^*)^{1/(3\nu-1)} \qquad c^* < c < 0.15\ \mathrm{g/cm^3} \quad (7)$$

where kT is the thermal energy, c is the concentration in solution (in mass/volume units), and c^* is the overlap threshold concentration defined by

$$c^* = 3(M_{PS}/N_{av})/(4\pi\langle s^2\rangle^{3/2}) \quad (8)$$

The proportionality constant k_{Π} reported is 2.2 for PS–toluene solutions[33] with $\nu = 0.595$. There can be differences among polymer systems in the value of K_{Π}, namely for PS and PI in toluene. (For example, poly(α-methylstyrenes) in toluene have slightly smaller ν (=0.585) and K_{Π} (=1.50).[32]) However, since the expansion factors (eqs 1 and 2) appear to be very similar for PS and PI in toluene, in the absence of more exact information, we take the two K_{Π} to be equal, too.

With this information, we can compare the osmotic free energy of the brush layers, $\Delta f_{r,ad}$, derived from the force–distance data, reduced to per unit mass, reduced by the thermal energy kT, and corrected for the differences between PS and PI in segment lengths, b, and monomer masses, m,

$$\Delta f_{r,ad} = \{[(m_B/N_{av})^{3\nu/(3\nu-1)}]/[wkT(4\pi b_B{}^3/3)^{1/(3\nu-1)}]\}(F/2\pi R) \quad (9)$$

with the osmotic free energy of homopolymer solutions, reduced and corrected in the same sense:

$$\Delta f_{r,os} = -\{[(m_B/N_{av})^{3\nu/(3\nu-1)}]/[wkT(4\pi b_B{}^3/3)^{1/(3\nu-1)}]\}\int \Pi[c(x)]\,dx \quad (10)$$

The prefactor in brackets in both eqs 9 and 10 is the correction required to scale together PS and PI for differences in segment length and monomer molecular weight suggested by eqs 7 and 8. The subscripts B refer to either PS or PI. The factor of 2π dividing F/R in eq 9 is that deriving from the Derjaguin analysis[23] for converting our force data to energy per unit area. The integral in eq 10 performs the same function for the osmotic pressure of the bulk solution; it calculates the work per unit area that would have to be done against osmotic pressure to concentrate the solution by compressing from large distances (effectively infinite separation is the lower limit of integration) down to some separation D ($D - L_{PVP}°$ is the upper limit of integration) where the concentration is higher. The integration of eq 10 can be carried out after inserting eq 7 for the osmotic pressure as a function of concentration, with the result

$$\Delta f_{r,os} = (3\nu - 1)K_{\Pi}c^{1/(3\nu-1)} \quad (11)$$

a function only of concentration in the semidilute range.

The comparison among our six sets of surface force data from Figure 1 on the different copolymers, replotted according to eq 9, is shown in Figure 2, along with the comparison to the bulk osmotic pressure data from eq 11. The data from different samples (different molecular weights and surface densities) diverge at low c (large D) but tend to merge toward a common line at high c (smaller D). In other words, $\Delta f_{r,ad}$ tends to become a function of concentration only, as is $\Delta f_{r,os}$. This lends support to the very basic molecular picture that purely osmotic interactions control the surface force profiles at high compression. Molecular weight and surface density are not important, except insofar as they are related to determining the average concentration in the gap between the mica sheets.

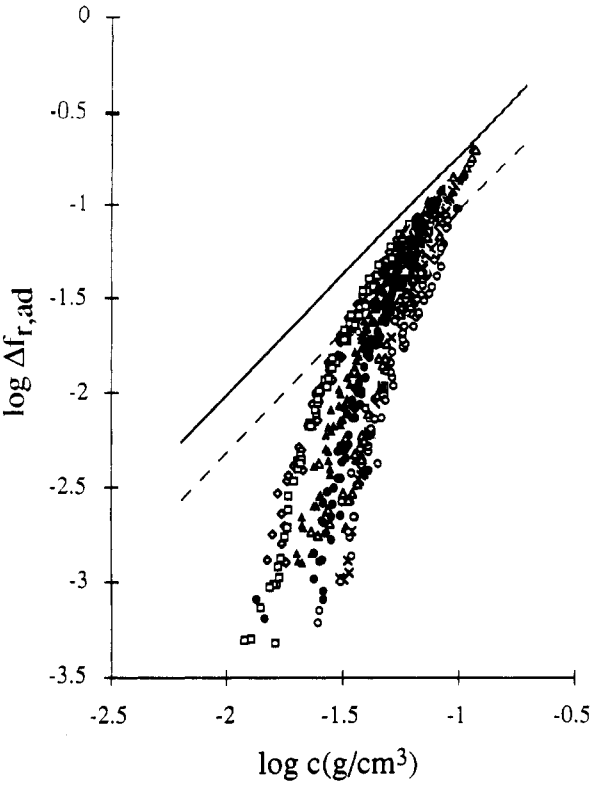

Figure 2. Comparison of the free energy of the adsorbed block copolymer layers (symbols) examined in Figure 1 and the osmotic free energy of semidilute homopolymer solutions (dashed line). The sense of the symbols is the same as in Figure 1. The dashed line represents the bulk osmotic pressure data of Noda and coworkers[32,33] plotted according to eq 11. The solid line is a guide to the eye, enabling an estimate of the high compression limit for the osmotic free energy of the copolymer layers, which is used for the comparison of the data and model in Figure 3.

Conversely, at the onset of interaction (large D or low c), average concentration in the gap is *not* the only important feature. At the onset of interaction, the stretched chain configuration of the individual brushes reduces the interaction energy well below that calculated from bulk osmotic pressure at lower, semidilute concentrations. Differences in chain stretching, related to the entropic elasticity of the chains, and depending on the configurations of the PS and PI chains, which, in turn, depend on chain length and surface density, reveal themselves at low compression in the divergence among the different sets of data in this limit. These experimental facts illustrate the basic physical ideas that have been predicted to control the structure of polymer brushes.[4,5,8,9]

Figure 2 also illustrates a quantitative discrepancy between the higher compression surface forces data and the higher concentration osmotic pressure data. $\Delta f_{r,ad}$ data for the adsorbed block copolymers tend to merge at a level a factor of about 2 higher (the solid line in Figure 2 represents this asymptotic limit approximately) than $\Delta f_{r,os}$ for the homopolymer solutions (the dotted line in Figure 2). This puzzling discrepancy might be related to a difference of chain conformation in bulk solutions and tethered brush layers.

In semidilute homopolymer solutions, the correlation length begins to decrease at the overlap concentration c^* as

$$\xi = R_F(c^*/c)^{\nu/(3\nu-1)} = \xi_0 c^{-\nu/(3\nu-1)} \quad (12)$$

where R_F is the root-mean-square end-to-end distance of the chain. The osmotic pressure of the solution is determined by and varies with the cube of ξ, and the value of ξ, in turn, relates to the segment–segment contacts that are determined by the chain conformation at a given concentration. The end-grafted chains in a brush layer certainly have conformations that are different from (and more constrained than) the conformation of free chains in the solution. Then, the scaling exponent of ξ ($-\nu/(3\nu-1)$) would be the same but its prefactor (ξ_0) might be somewhat smaller in a brush layer than in a homopolymer solution of the same c, as is in fact suggested from Figure 2. Although the origin of the difference of ξ_0 (and thus of $\Delta f_{r,os}$ and $\Delta f_{r,ad}$ at high compression) for the homopolymer solution and brush layer is still a puzzling problem that requires more study, we keep this difference in our mind and compare the surface force data with theoretical models in the following section.

Comparison with Models for Force–Distance Profiles. In order to understand the relationship among the different sets of data for different molecular weight and surface densities in Figure 1 in more detail, we can compare the data with models of the force–distance profiles of tethered brushes.[6,8,9] The simplest analytical forms of these models have been developed for end-grafted layers of sufficiently high densities and marginally good solvents so that the layers were effectively in a mean-field regime. In the experiments reported here, we are clearly outside of this regime on several counts. The data on adsorbed amount and molecular size in the experimental section show that the brushes created by the nonadsorbing blocks are not very highly overlapping. Furthermore, toluene is a very good solvent for both nonadsorbing blocks so that excluded volume correlations cannot be safely ignored. We shall therefore compare the data with theoretical models encompassing these effects.

The first model inviting comparison with these data is that of Patel et al.[9] where excluded volume effects are treated but the density profile of segments within the brush is assumed to be constant (that is, a step-function profile). In this respect, it is the direct extension of the Alexander–de Gennes model of single brushes to two interacting brushes. It is also related to a model of interacting brushes proposed by de Gennes.[8] We shall term the model of Patel et al.[9] the PTH model and redevelop it here in a form most suitable for comparison with the data. We aim to put in quantitative estimates of the coefficients of the terms in the PTH model.

The PTH model uses the essential Alexander–de Gennes idea that the equilibrium interaction between two proximal brushes is determined by the balance between the osmotic and elastic energies of the brushes. The basis on which we will write the model is first in terms of the energy of one tethered layer per unit area. On this basis, the osmotic free energy reads

$$f_{os} = (3\nu-1)kTK_\Pi(c/\beta)^{1/(3\nu-1)}(\sigma M_B/N_{av})^{-3\nu/(3\nu-1)}(4\pi b_B{}^3/3)^{1/(3\nu-1)} \quad (13)$$

which is essentially identical to eq 11 except that the kT unit is involved, the basis has been changed from per unit mass to unit area, and the empirical factor β has been introduced to account for the experimental observation, in Figure 2 and discussed above, that there is a quantitative discrepancy in the high compression limit between the force data and the solution data on osmotic pressure. $\beta^{\nu/\nu p-1}\xi = \xi_{ad}$ with ξ and ξ_{ad} being the correlation lengths in a homopolymer solution and a polymer brush of the same c (see eq 12). If we take $\beta = 1$, we are estimating the magnitude of the osmotic free energy contribution purely from bulk solution data; if we adjust β, we can choose it to agree with the force data in the osmotic regime by selecting a value of β less than 1. In eq 13, and the equations that follow, the subscript B is used to designate the polymer type, either PS or PI.

In the elastic term, the tethered block, experiencing excluded volume interactions, is modeled as a Gaussian chain of $n = N(\xi/a)^{-1/\nu}$ blobs with step length ξ. Excluded volume operates within these blobs, but there are no correlations among the blobs. The effective step length of a monomer ($a \approx 6^{1/2}b$) is defined by the relation $R_F = aN^\nu$. The elastic energy per unit area of these tethered chains is given by

$$f_{el} = (3/2)kT\sigma L^2/(n\xi^2) \quad (14)$$

or, converting the correlation length into concentration in the tethered layer with the use of eq 12

$$f_{el} = (kT/4b_B{}^2)(L^2/N_B)\sigma(c/\beta)^{(2\nu-1)/(3\nu-1)}(m_B/N_{av})^{-(2\nu-1)/(3\nu-1)}(4\pi b_B{}^3/3)^{(2\nu-1)/(3\nu-1)} \quad (15)$$

Minimization of the total free energy, $f = f_{os} + f_{el}$, with respect to L gives the equilibrium thickness of a single layer, including numerical coefficients and exponents derived from the data

$$L_{eq} = \{[4(3\nu-1)K_\Pi]/(4\nu-1)\}^{(3\nu-1)/4\nu}[4\pi\sigma/3\beta]^{(1-\nu)/2\nu}b_B{}^{1/\nu}N_B \quad (16)$$

Stretching in the equilibrium configurations of these end-anchored chains is indicated by eq 16 both in the magnitude of L compared to R_F and in the fact that the end-anchoring produces a linear, rather than square-root, scaling of L with N.

For two layers of tethered chains interacting with one another, an additional physical assumption goes into the PTH model,[8,9] namely that the two layers do not interpenetrate one another on squeezing. The degree of this interpenetration is an interesting issue in itself, which has been discussed rather extensively recently.[8,35] Interpenetration controls the degree of entanglement possible between two brushes and therefore should be significant in the dynamic properties of polymeric systems containing polymer brushes. The basic argument that the degree of interpenetration should be low is related directly to the stretched configuration of the single brush found in eq 16. The single, dense brush is stretched at equilibrium owing to its tendency to dilute itself, thereby lowering the osmotic pressure interactions in the brush. When confronted with an opposing brush, the driving force for stretching is diminished. As compression increases, the average density of segments, and therefore the osmotic interactions, are imposed on the chains. Stretching so as to penetrate into the other brush is useless in diminishing osmotic pressure. The originally stretched chains therefore shrink back toward their unstretched dimensions. We will discuss the idea of noninterpenetration in more detail in a subsequent section.

From the point of view of modeling two interacting brushes, the noninterpenetration idea provides a great simplification. In this case the thickness, L, of one brush

interacting with an impenetrable second brush is just half the separation between the solid surfaces to which the layers are tethered (minus the small correction for the thickness of the anchoring blocks): $D/2 - L_{PVP}°$. Thus, eqs 13–16 are converted in the PTH model directly into an expression for the total free energy per unit area as a function of separation for two interacting layers. Then, with the Derjaguin approximation for relating force to energy per unit area,[23] the model for the force versus distance profiles is developed. These are conveniently expressed in terms of dimensionless, reduced force, **f**

$$\mathbf{f} = (F/R)[kT\sigma^{(2\nu+1)/2\nu}b_B^{1/\nu}N_B] \quad (17)$$

and reduced distance, ∂:

$$\partial = [D - 2L_{PVP}°]/[2\sigma^{(1-\nu)/2\nu}b_B^{1/\nu}N_B] \quad (18)$$

The reduced force is (4π times) the measured interaction energy per unit area divided by the energy per unit area (energy per blob times the number of blobs per unit area) in the uncompressed, infinite separation brushes. The reduced distance is the separation between the surfaces to which the nonadsorbing blocks are attached, $(D - 2L_{PVP}°)/2$, divided by $L_{eq}/\{[4(3\nu - 1)K_\Pi](4\nu - 1)\}^{(3\nu-1)/4\nu}[4\pi/3\beta]^{(1-\nu)/2\nu}$, which is approximately $L_{eq}/4$ for the experimental constants applicable to these data. Therefore, when we present data in the scaled format subsequently, the onset of interaction will occur at about $\partial = 4$.

In terms of these reduced quantities, the PTH model[9] combines eqs 13–18 into a universal, dimensionless force–distance profile:

$$\mathbf{f} = X\{[Y\partial^{-1/(3\nu-1)} - 1] + (4\nu - 1)^{-1}[Z\partial^{(4\nu-1)/(3\nu-1)} - 1]\} \quad (19)$$

where X, Y, and Z are collections of experimental constants:

$$X = 4\pi[(4\nu - 1)/4]^{1/4\nu}[(3\nu - 1)K_\Pi]^{(4\nu-1)/4\nu}(4\pi/3\beta)^{1/2\nu} \quad (20)$$

$$Y = \{[4(3\nu - 1)K_\Pi]/[(4\nu - 1)]\}^{1/4\nu}(4\pi/3\beta)^{(1-\nu)/2\nu(3\nu-1)} \quad (21)$$

$$Z = \{[4(3\nu - 1)K_\Pi]/[(4\nu - 1)]\}^{-(4\nu-1)/4\nu}(4\pi/3\beta)^{-(1-\nu)(4\nu-1)/2\nu(3\nu-1)} \quad (22)$$

In eq 19, the first term represents the effects of the osmotic interactions resisting compression; the second term accounts for the effects of elasticity resisting chain stretching. All of the quantities, except β, involved in eqs 19–22 are directly determined by independent experiments. In this feature, these equations differ from the original formulation of the PTH model. The additional constant β is used to account for the effects of the discrepancy with bulk osmotic pressure data idscussed in connection with Figure 2.

Figure 3 compares the data shown in Figure 1 with the model prediction (eq 19) in reduced form. The dotted line is the prediction of the model with $\beta = 1$ (with no correction for the discrepancy with bulk osmotic pressure); the solid line is that with $\beta = 0.58$ which corresponds to the solid line indicated in Figure 2 (the apparent high compression asymptote of $\Delta f_{r,ad}$). Figure 3 shows that correcting $\Delta f_{r,os}$ by this factor in the formulation of the model for the force–distance profile gives good agreement with the data.

In Figure 3, we note that the data for the block copolymer layers having different N, σ, and chemical composition (PI and PS) are well-collapsed in a single curve with the reduced variables **f** and ∂. While there remains a certain

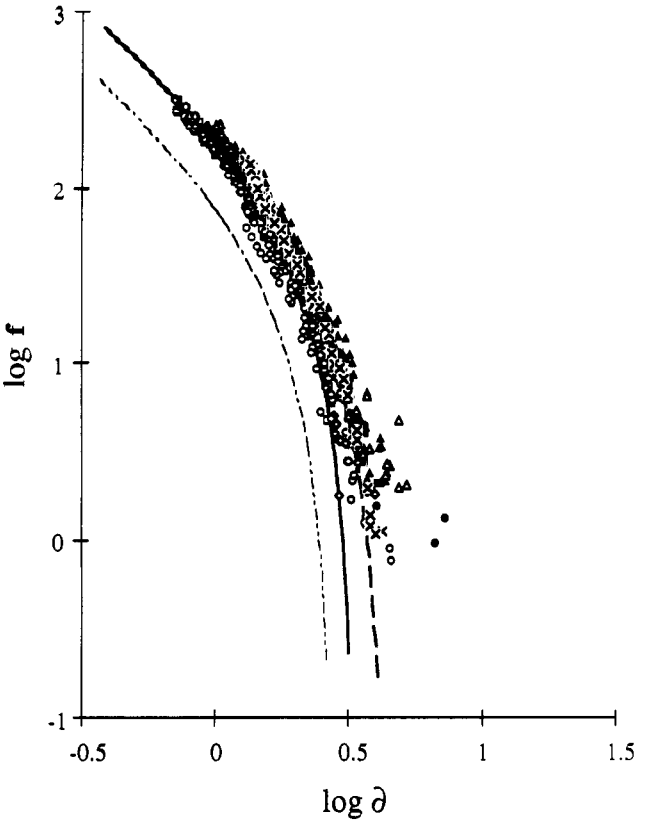

Figure 3. Comparison of the surface force data (symbols) and the prediction of the model of Patel et al.[9] (thin dotted line for $\beta = 1$ and thick solid line for $\beta = 0.58$; see text) on double logarithmic scales. The sense of the symbols is the same as in Figure 1. The thick dashed line indicates the prediction of the model of Milner et al.[6] with $\beta = 0.58$.

dispersion in the plot, it is not systematic with respect to tethered chain length, surface density, or chain type. Some of this small dispersion may be due to our lack of accounting for the swelling of the PVP anchor blocks or the fact that the covalent bond joining the anchor and the nonadsorbing block is not rigidly fixed at a precise elevation above the mica surface. The point of onset of detectable forces is particularly well-scaled through the reduced variable ∂.

Concerning the form of the universal force–distance profile, we see that the PTH model underestimates **f** if the overlap threshold for bulk homopolymer solutions ($\beta = 1$, dotted curve) is used in the model. On the other hand, quantitative agreement is seen between the model with $\beta = 0.58$ and the data at compression greater than $\mathbf{f} \approx 10$. In some sense, this means that the PTH model agrees well with the force–distance data at intermediate compressions if the osmotic free energy term is estimated from *data* at high compressions.

As can be seen clearly from the double logarithmic plot of Figure 3, the PTH model underestimates **f** for larger ∂, even with $\beta = 0.58$. This kind of discrepancy has been noted in previous comparisons of force data with theory.[36] It appears that the step-function density profile assumed in the PTH model becomes a poorer approximation for larger ∂. Naturally, given its character, this model works better when D is smaller and the segment density in the gap is fairly uniform.

Milner et al.[6] have developed a model (MWC) that treats the segment density profile in the tethered brush more realistically. Osmotic and elastic contributions to the free energy are still the ingredients of the model. In the MWC model, however, the balance between osmotic repulsion and elasstic resistance is done locally, at each point along the chain, and self-consistently, in contrast to the PTH

model which assumes that every chain is equally stretched and balances effects over the chain as a whole. The MWC model is based on a less restrictive assumption than uniform stretching; namely, it assumes that every region of the chain is strongly stretched locally to the point that fluctuations around the most probable chain trajectory are unimportant. This model produces a segment density distribution that varies with distance from the tethering surface.

In the simplest form, applicable to the moderately high density of end-anchored chains and weak excluded volume effects, this type of model can be solved analytically[6,37] to give a parabolic dependence of the segment density on distance from the anchoring surface. That form of the model does not apply strictly to the data here, which are subject to stronger excluded volume correlations, for the same reasons that the PTH model had to be modified. Milner et al.[6] also developed a form of the model appropriate for semidilute cases with excluded volume. As in the PTH model, the MWC model predicts a universal form of the relationship between $\mathbf{f}$ (eq 17) and ∂ (eq 18) for forces in semidilute good solvents, although that relationship cannot be expressed in a compact, analytical form. We have evaluated it numerically by following the procedure developed by Milner et al.[6]

In Figure 3, the heavier, dashed line indicates the free energy calculated from the MWC semidilute model using parameters equivalent to the PTH model with $\beta = 0.58$. These two models converge in the high compression limit since, in this region of compression, the more detailed treatment of stretching by MWC, and the resultant differences in the segment density profiles between the two models, have been rendered irrelevant by the imposition of confinement by squeezing the layers and the consxequent uniform segment density in the gap. On the other hand, in the larger ∂ limit, corresponding to $\mathbf{f}$ less than about 10, the MWC agrees better with the data plotted in this universal format. The nearly parabolic profile predicted by the MWC model is necessary for an accurate prediction of the onset of repulsive forces in the weak compression regime. We point out again that, apart from the factor β which is necessary to make the high compression data coincide with the osmotic pressure of a free solution, the form of the MWC model we apply has no adjustable parameters. All constants are determined independently by our measurements of chain length and surface density of adsorbed chains.

The double logarithmic plot of Figure 3 also shows that, at the very weakest compressions, there is the most dispersion of the data sets from one another and from the universal format. These are the data that we measure with the least precision, so we should avoid attributing too much significance to them. However, there are some additional, real effects anticipated to occur in this region which may be relevant and should be mentioned. First of all, the local, strong-stretching assumption embodied in the MWC model must breakdown at the periphery of the brush where the segment density becomes sufficiently low so that the osmotic interactions no longer generate stretching. This feature was evident in the calculations of Hirz and others[6] where a "tail" of apparently exponential form is expected. Milner[11] discusses this region in detail; we only mention it here to bring attention to the fact that universal MWC behavior is not expected for very weak compression.

This region is of considerable practical interest since, whereas the denser, inner brush is largely impenetrable because it is stretched, the periphery is penetrable and therefore is in a position to control the amount of entanglement with a brush. In addition to the effects of tails, effects of even small polydispersity should be considered.[6] Milner has suggested that they are important in quantitative comparisons.[36] In our case, even if we had perfect monodispersity, the fact that the covalent links between the nonadsorbing and adsorbing blocks could occupy a small range of positions above the mica surface could produce an apparent polydispersity in the length of the tethered chains, since some would be able to reach farther out from the surface by virtue of their anchoring position. None of these effects are important in the higher compression regime and, quantitatively, do not seem to be very large, even in the weaker compression regime of our data.

Force–Distance Profiles for Asymmetric Layers. For asymmetric layers, each one composed of a different species 1 and 2, the Derjaguin analysis[23] relates the measured quantity $F(D)/R$ to the free energy $f_i(D)$ of the layers i (=1, 2) per unit area by

$$F(D)/R = 2\pi[f_1(L_1) + f_2(L_1) - f_1(L_{1,eq}) - f_2(L_{2,eq})] \qquad D = L_1 + L_2 \quad (23)$$

where L_i is the thickness of the compressed layer i and $L_{i,eq}$ is the equilibrium thickness for that layer. Thus, independently of any molecular model, we can compare the F/R data for the asymmetric interactions with expectations based on the measured symmetric interactions *assuming*, in developing these expectations, that (1) there is no penetration between the layers in either the symmetric or asymmetric cases and (2) the chain configuration and segment density profile (and hence the free energy) in a layer i are determined only by the thickness, L_i, of that layer, and are the same for the symmetric and asymmetric cases when L_i is the same. With these assumptions, the minimization of the free energy of an arbitrary two-layer, interacting system gives

$$F_a(D)/R = (1/2)[F_1(D_1)/R + F_2(D_2)/R] \qquad 2D = D_1 + D_2 \quad (24)$$

$$\partial[F_1(D_1)/R]/\partial D_1 = \partial[F_2(D_2)/R]/\partial D_2 \qquad 2D = D_1 + D_2 \quad (25)$$

where the subscripts 1, 2, and a stand for the symmetric layers of the copolymers 1 and 2, and the asymmetric layers, respectively. When the two layers are chemically identical, eq 25 may be rewritten in terms of the reduced free energy of symmetrical interactions, $\Delta f_{r,ad}$ (cf., eq 9 and Figure 2), and the concentration in respective layers, c, as

$$[\partial \Delta f_{r,ad}/\partial(1/c)]_1 = [\partial \Delta f_{r,ad}/\partial(1/c)]_2 \quad (25')$$

(Here we have assumed $D \gg L_{PVP}$; cf., eq 6.)

The minimization calculation for $F_a(D)/R$ based on the symmetric layer data of Figure 1, and the above assumptions, was carried out in two ways. The first was the direct numerical differentiation according to eq 25. The second method we employed, since we were concerned about possible numerical errors with the first, was to scan the values of D_i in the $F_i(D_i)/R$ data, under the constraint $2D = D_1 + D_2$ to determine the minimum of the sum $F_1(D_1)/R + F_2(D_2)/R$. The results of those two methods were in good agreement.

Among the polymers for which data on symmetric interactions are presented in Figure 1, three different kinds of asymmetric interactions can be studied: *chemical*, where one brush is PS and the other is PI; *molecular weight*,

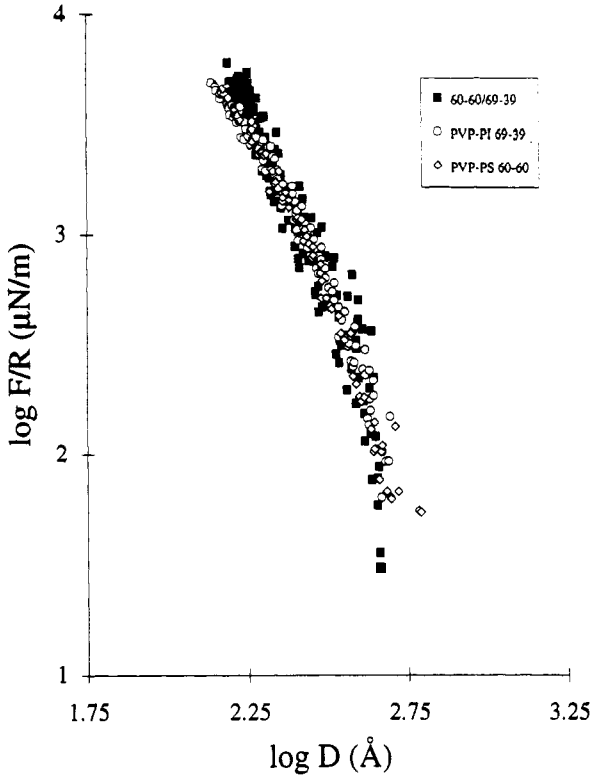

Figure 4. Data on chemical asymmetric interaction. Symmetric interactions between PVP–PS and between PVP–PI layers compared with asymmetric interactions between the two. All data were obtained in toluene at 32 °C.

where chains of the same type and the same number per unit area but of different lengths; *structural*, where again the chains are of the same type but now with different numbers of chains per unit area in each brush. The polymers of Figure 1 provide pairs where each of these effects can be studied separately.

We examine the case of chemical asymmetry first. Figure 1 shows that the symmetric force curves for PVP–PI 69–39 and for PVP–PS 60–60 are nearly identical. Moreover, the surface densities measured, reported in Table II, for these two polymers are very close. This is to be expected since the size of the anchors and the coil dimension of nonadsorbing blocks are quite close. The study of this asymmetrical interaction would permit the observation of any additional interaction force due to the chemical dissimilarity of PI and PS, a pair of polymers that are strongly immiscible in bulk and phase separate in toluene even at low concentration. Figure 4 shows the data on this asymmetric interaction, superimposed on the two symmetric interaction curves, where it is readily seen that there is no significant difference among the three of them.

While at first blush, this result may seem surprising, we believe that it is exactly what one should expect given the idea that polymer brushes are scarcely penetrable. In fact, the similarity among these three curves is certainly consistent with impenetrability. If there is little penetration between similar (symmetric) layers, one should not expect there to be an appreciable effect of increasing the repulsion between the brushes further by making them chemically dissimilar.

The effect of molecular weight asymmetry is illustrated in Figure 5. The force–distance profiles for the symmetric interactions for PVP–PS 60–60 and PVP–PS 60–90 are illustrated by the two broken lines. Table II shows that these polymers have very close values of surface density. The data agree reasonably well with the expectations of

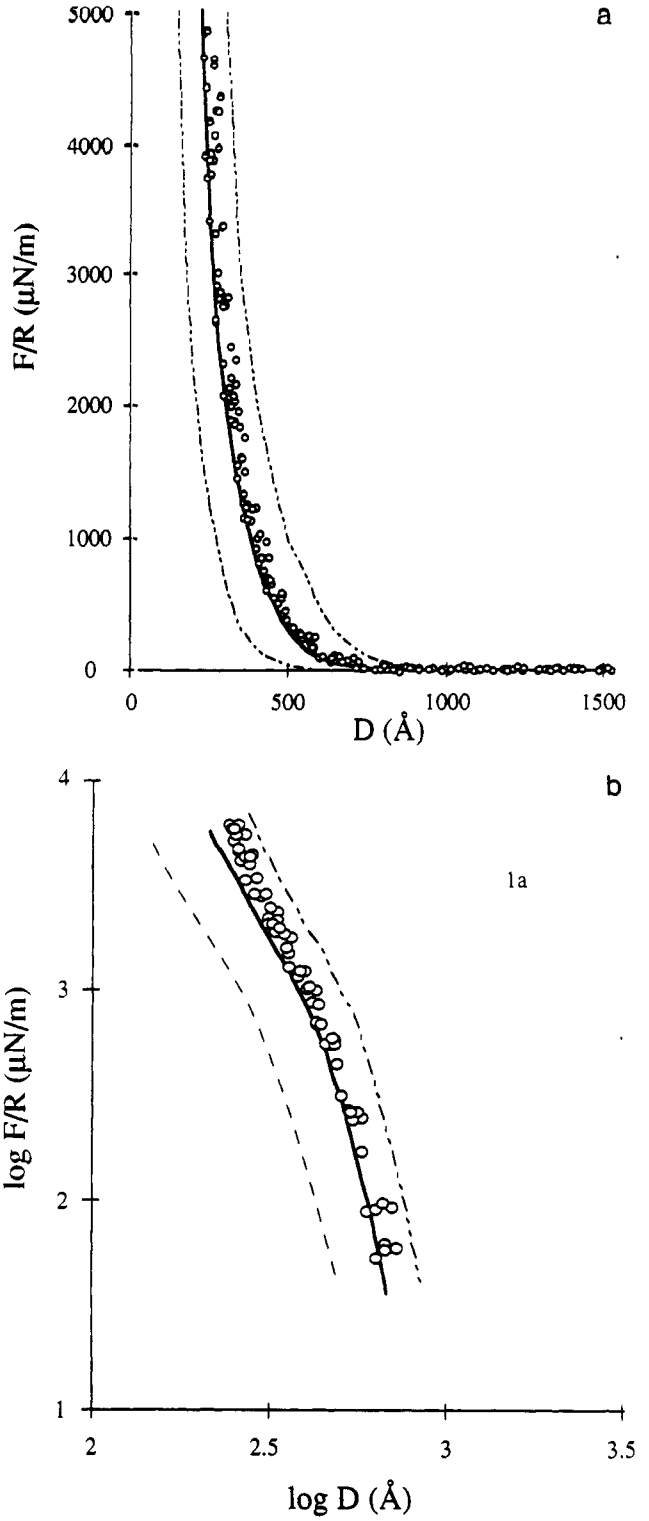

Figure 5. Data on molecular weight asymmetric interaction. Force–distance profiles for asymmetric interaction of layers of PVP–PS 60–60 and 60–90 copolymers obtained in toluene at 32 °C. The longer-ranged and the shorter-ranged dashed lines represent the two symmetric interactions. The solid line is the prediction of the bisection rule (see text).

eqs 24 and 25, which has been called a "bisection rule",[38] where impenetrability is still an essential ingredient. The two brushes of different heights meet at the position corresponding to the sum of the two single brush heights. On further compression, the force–distance profile follows closely the curve predicted on the basis that the two layers compress individually without interpenetrating one another more than they did with themselves in the symmetric experiment. The data actually tend to be slightly, but systematically, on the high side of this prediction. This

could be due to the fact that the small degree of penetrability of each of the two brushes would not be expected to be exactly equal. At equal density of tethered chains, the depth of the interpenetrating region, δ, relative to the equilibrium layer thickness L_{eq} (eq 16), should vary with chain length as $\delta/L_{eq} \sim N^{-2/3}$.[35] Thus, the larger brush is less penetrable, as gauged by the penetrable fraction of its total height. This could account for the small deviation from the bisection rule in Figure 5.

Figure 6 compares the force–distance data obtained for the PVP–PI 30–217/26–50 asymmetric pair interaction with the prediction of eqs 24 and 25. In this case, we have chemically identical blocks, as in Figure 5; however, both the chain length *and* the surface density are different on the two opposing surfaces. In fact, the surface density of the higher molecular weight polymer is lower by nearly the same proportion as the ratio of the chain lengths of the PI blocks, leading to the interesting situation that the two surfaces have a similar number of segments tethered to them but, on one side they are in a looser, softer brush, while on the other side they are in a denser, stiffer brush. These data deviate noticeably from the bisection rule (indicated by the solid curve). Whereas the onset of the interaction occurs at a separation equal to the sum of the two individual brush heights, the rise in the forces with further compression is softer than that anticipated from the noninterpenetration idea. The repulsive force observed is smaller by a factor of about 2 at intermediate separation. The difference between the actual data and the bisection rule is the largest at intermediate D and decreases at smaller separations.

A distinction to be drawn between the results of Figures 5 and 6 is that of the concentrations of segments within the opposing brushes, c_1 and c_2. In the range of D examined, c_1 and c_2 calculated under the assumption of impenetrability (cf., eqs 24–25′) are almost equal in the first case, and unequal in the second case. This difference of the two cases is naturally expected from the reduced free energies of *symmetrical* interactions, $\Delta f_{r,ad}$, that are summarized in Figure 2.

For the first case, the PVP–PS 60–60 and 60–90 layers of the same concentrations have indistinguishable $\Delta f_{r,ad}$ in the entire range of D examined (cf., unfilled triangles and crosses in Figure 2). Thus, the free energy of asymmetric interaction is minimized at $c_1 = c_2$ (cf., eq 25′), even when the compression is weak and the elastic free energy still contributes to $\Delta f_{r,ad}$. On the other hand, for the second case, the PVP–PI 26–50 and 30–217 layers of the same concentration have different $\Delta f_{r,ad}$ (cf., unfilled circles and squares in Figure 2). This difference, due to the elastic contribution, becomes smaller for smaller D but still remains even at the highest compression examined in Figures 2 and 6. Under the assumption of impenetrability, the free energy minimization for such asymmetric layers leads to $c_1 \neq c_2$ (cf., eq 25′): It leads to $c_1 = c_2$ only when the elastic contribution vanishes at much higher compression (not achieved in this study).

For the first case with $c_1 = c_2$, there would be little driving force to overcome the impenetrability, and we naturally expect the bisection rule to hold. On the other hand, for the second case, unequal concentrations in the opposing brushes would create this driving force. We could imagine the following hypothetical experiment. If we insert an impermeable membrane between the layers, the bisection rule should hold but the concentrations on either side of the membrane are unequal. In such cases, the removal of the membrane (corresponding to the real situation in our experiments) should be expected to induce some interpenetration and/or rearrangement of chain configuration so that the concentration mismatch is diminished. Then, too, the forces between the two layers should be expected to decrease somewhat from the bisection rule prediction. This is what we observe in Figure 6. Shim and Cates[38] have made self-consistent field calculations to examine some situations of structural asymmetry: they conclude that interpenetrability softens the force profile; however, at the degree of precision for which they calculated the

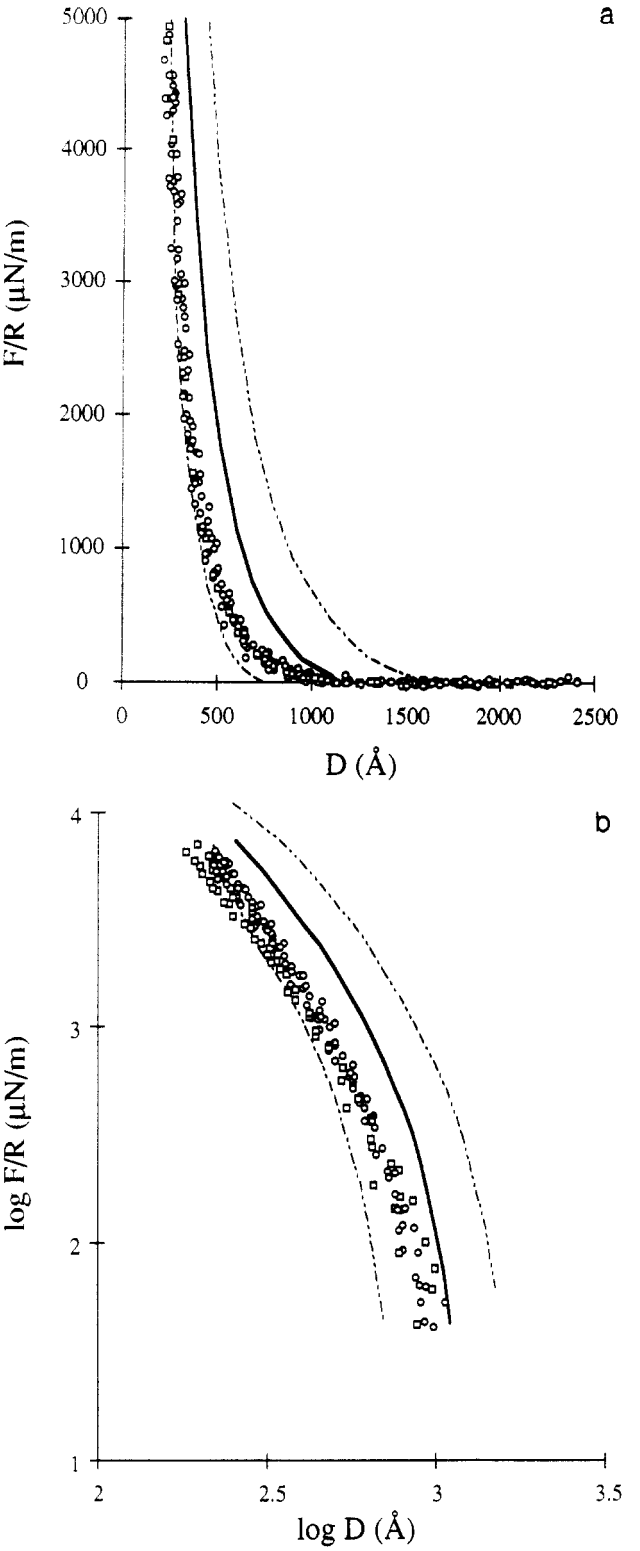

Figure 6. Data on structural asymmetric interaction. Force–distance profiles for asymmetric interaction of layers of PVP–PI 30–217 and 26–50 copolymers obtained in toluene at 32 °C. The longer-ranged and the shorter-ranged dashed lines represent the two symmetric interactions. The solid line is the prediction of the bisection rule (see text).

profiles (they calculated force profiles spanning 6 orders of magnitude in force), they could not see a large difference in penetrability produced by structural asymmetry. This issue deserves further attention.

Adhesion of Dry Block Copolymer Layers. A typical fringe shape observed when the dry surfaces were in adhesive contact is illustrated in Figure 7. This fringe shape appeared spontaneously on initial approach of the two PI surfaces but required compression of the PS surfaces, as described in the Experimental Section. This is typical of the fringe shape when no external load is applied to the two surfaces in contact. On application of a tensile force (i.e., in the direction tending to separate the surfaces), the contact area, observed as the measured size of the flat part of the fringe, diminished until the two surfaces jumped apart from a finite area of contact, as predicted by the JKR theory.[26] The shape of the fringes at zero load is predicted by the JKR theory to be

$$h' = (\rho'^2 - 1)^{1/2} + (\rho'^2 - 2/3)\tan^{-1}(\rho'^2 - 1)^{1/2} \quad (26)$$

where $h' = h\pi R/a_c^2$ and $\rho' = \rho/a_c$, with h being the separation at a certain radial position ρ from the center of contact and a_c being the area of the contact between the two surfaces. Figure 7 compares the measured fringe shape with this prediction; the agreement seems to be reasonably good. This has been found to be the case for measurements of the contact shape between other materials as well.[25,27] On this basis, we have used the JKR theory to convert our measurements of pull-off force (or the force required to separate the surfaces, F_s) to adhesive energy.

According to the JKR theory, the adhesive energy, γ, is related to the pull-off force by

$$\gamma = F_s/3\pi R \quad (27)$$

On the basis of this equation, the adhesive energy was determined to be

$$\gamma = 25 \pm 5 \text{ mJ/m}^2 \text{ for PVP–PS 60–60}$$

$$\gamma = 55 \pm 10 \text{ mJ/m}^2 \text{ for PVP–PI 30–217}$$

Independent measurements have established[22] that when adsorbed layers such as these are dried, there is good vertical separation of the PS (or PI) from the PVP, so that we may accurately presume that the contact we are measuring is between two PS or PI surfaces. These numbers may then be compared with the literature values of the surface energies of PS and PI, which are 30 ± 5 mJ/m^2 for PS and 34 ± 3 mJ/m^2 for PI.[39]

If the contact between the two layes in the surface forces apparatus produces only a reversible decrease in surface area of the two layers of material, but no interpenetration or rearrangement, they γ is expected to be equal to the thermodynamic surface energy of the polymer. In comparing our data with literature surface energies, we see that, for PS, there is close agreement; however, for PI, the energy from the pull-off force is significantly larger than the literature surface energy.

PS is glassy under the conditions of our experiment, so that it is reasonable to suppose that there is molecular contact but no interpenetration between the dry PS layers. Measurement of the surface energy of a solid PS film by reversible contacting in the surface apparatus is similar in spirit to the measurements of the surface energy of solid polymers developed by Merrill et al.[27] where the mica itself is replaced by a thin solid polymer rather than coated with it, as we have done here. Both methods may be usefully pursued as avenues to solid surface energies.

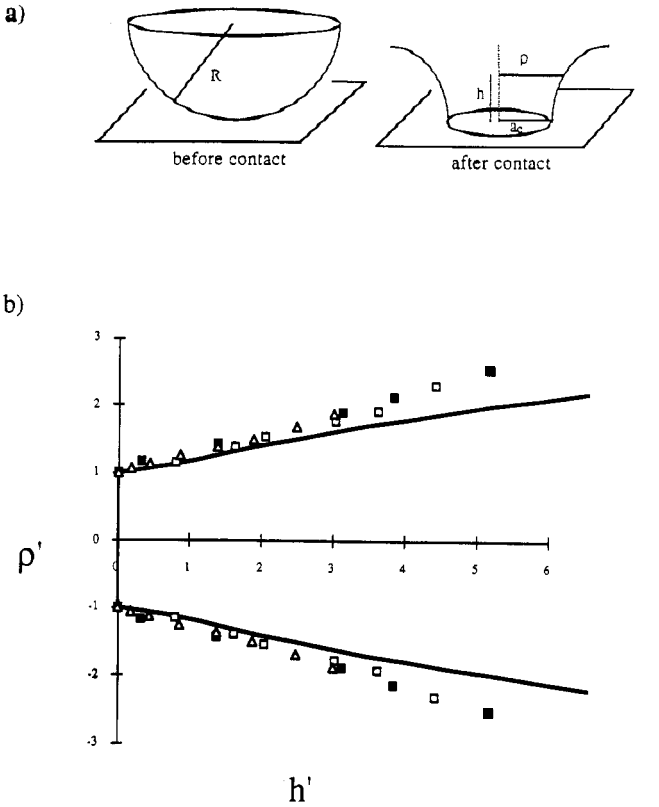

Figure 7. (a) Schematic diagram for the surface of dry block copolymer layers before and after contact. (b) Comparison of the surface profile for PVP–PI 26–50 copolymer obtained at 32 °C with the prediction of JKR theory.[26] The three symbols indicate the surface profiles obtained for three contact spots having different values for R and a_c.

PI is well above its glass transition at the temperatures we have used (32 °C), so that it is reasonable here to expect the thin, dry PI surfaces to rearrange and interpenetrate on contact. The energy values that we measure, higher than reported surface energies, certainly reflect this interpenetration. One possibility is that the configurational constraint of the PI chains, confined to a film smaller than their natural molecular dimensions, is partially released on contact since the chains can expand by interpenetration into twice their volume, giving rising to a drop in the total energy of the two layers on contact. Interpenetration could also introduce nonequilibrium contributions to the pull-off energy, such as energy dissipation on pull-off due to disengagement. In this connection, it is important to note that we could observe no dependence of the pull-off force on time in contact from a few seconds to times of order 1 h.

Conclusions

We have measured the surface forces and the grafting densities for several PVP–PI and PVP–PS block copolymer layers adsorbed on mica in toluene. All of the force versus distance data on six pairs of symmetrical interactions collapse with reasonable accuracy in a reduced plot, the variables of which are suggested by models developed by Patel et al.[9] and by Milner et al.[6] The shape of this curve is predicted with reasonable accuracy by both models, with an advantage to the latter. There are no free parameters in this comparison. Quantitatively, with our estimates of the necessary parameters, both models underpredict the force and its range by a factor of about 2. This difference seems to be related to a difference of osmotic pressure in the adsorbed layer and homopolymer solution of the same concentration.

The surface density data in Table II show that none of these layers are *very* strongly into the overlap or brush regime. It is interesting then to note how well these brush-type models do in representing the data. It is also a testimony to the power of the models that the form of the data on two very different types of tethered chains, PS and PI, is virtually identical.

One aspect of tailoring interactions between layers of polymeric amphiphiles such as these has also been explored in this work, namely, asymmetric interaction between two different layers. Chemical, molecular weight, and structural asymmetries were all studied. These data produced additional support for the idea that even relatively sparse brushes are scarcely penetrable by a chain coming from outside. Future directions in tailoring these interactions will include the study of controlled distribution in the molecular weights of the tethered chains (e.g., bimodal brushes[40]) and interactions among the tethered chains other than excluded volume (e.g., electrostatic interactions in tethered polyelectrolytes[41]).

Acknowledgment. We would like to acknowledge, with appreciation, financial support of this work from several sources: the National Science Foundation [NSF/CTS-9107025, Interfacial Transport and Separations Program (CTS) and Polymers Program (DMR) and NSF/INT-9016735, U.S.-Japan Cooperative Research Program (INT)], the Japan Society for the Promotion of Science (Grant No. ENGR-194), and the Petroleum Research Fund, administered by the Americal Chemical Society. Many discussions and interactions with colleagues have been very helpful in pursuing this work. These colleagues include Sanjay Patel, Michael Cates, Edward Parsonage, Scott Milner, Tom Witten, and Georges Hadziioannou.

References and Notes

(1) Halperin, A.; Tirrell, M.; Lodge, T. *Adv. Polymer Sci.* **1992**, *100*, 31.
(2) Milner, S. T. *Science* **1991**, *251*, 905.
(3) Marques, C. M.; Joanny, J.-F.; Leibler, L. *Macromolecules* **1988**, *21*, 1051.
(4) Alexander, S. *J. Phys. (Paris)* **1977**, *38*, 977 & 983.
(5) de Gennes, P.-G. *J. Phys. (Paris)* **1976**, *37*, 1443; *Macromolecules* **1980**, *13*, 1069.
(6) Milner, S. T.; Witten, T. A.; Cates, M. E. *Macromolecules* **1988**, *21*, 2610; *Europhys. Lett.* **1988**, *5*, 413; *Macromolecules* **1989**, *22*, 853. Milner, S. T.; Wang, Z. G.; Witten, T. A. *Macromolecules* **1989**, *22*, 489. Hirz, S. J., M.S. Thesis, University of Minnesota, 1986. Skvortsov, A. M.; Pavlushkov, I. V.; Gorbunov, A. A.; Zhulina, E. B.; Borisov, O. V.; Pryamitsin, V. A. *Polym. Sci. USSR (Engl. Transl.)* **1988**, *30*, 1706.
(7) Shim, D. F. K.; Cates, M. E. *J. Phys. (Paris)* **1989**, *50*, 3535.
(8) de Gennes, P.-G. *C.R. Acad. Sci., Ser. 2* **1985**, *300*, 839.
(9) Patel, S.; Tirrell, M.; Hadziioannou, G. *Colloids Surf.* **1988**, *31*, 157.
(10) Patel, S.; Tirrell, M. *Annu. Rev. Phys. Chem.* **1989**, *40*, 597.
(11) Milner, S. T. *J. Chem. Soc., Faraday Trans. 1* **1990**, *86*, 1349.
(12) Croucher, M. D.; Hair, M. L. *Colloids Surf.* **1980**, *1*, 349.
(13) Hadziioannou, G.; Patel, S.; Granick, S.; Tirrell, M. *J. Am. Chem. Soc.* **1986**, *108*, 2869.
(14) Fujimoto, T.; Nagasawa, M. *Advanced Techniques for Polymer Synthesis*; Kagaku-Dojin: Kyoto, 1972. Fujimoto, T. Personal communication.
(15) Morton, M.; Fetters, L. *Rubber Chem. Technol.* **1975**, *48*, 359.
(16) Arai, K.; Kotaka, T.; Kitano, Y.; Yoshimura, K. *Macromolecules* **1980**, *13*, 1670. Kudose, I.; Kotaka, T. *Macromolecules* **1984**, *17*, 2325.
(17) Imanishi, Y. M.S. Dissertation, Osaka University, 1987.
(18) Yoshida, H.; Watanabe, H.; Adachi, K.; Kotaka, T. *Macromolecules* **1991**, *24*, 2981.
(19) Israelachvili, J. N.; Adams, G. E. *J. Chem. Soc., Faraday Trans. 1* **1978**, *74*, 975.
(20) Tirrell, M.; Patel, S.; Hadziioannou, G. *Proc. Natl. Acad. Sci. U.S.A.* **1987**, *84*, 4725.
(21) Patel, S. S. Ph.D. Dissertation, University of Minnesota, 1988.
(22) Parsonage, E. E.; Tirrell, M.; Watanabe, H.; Nuzzo, R. G. *Macromolecules* **1991**, *24*, 1987.
(23) Derjaguin, B. V. *Kolloid. Z.* **1934**, *69*, 155.
(24) Israelachvili, J. N. *Intermolecular and Surface Forces*, 2nd ed.; Academic Press: San Diego, 1991.
(25) Horn, R. G.; Israelachvili, J. N.; Pribac, F. *J. Colloid Interface Sci.* **1987**, *115*, 480.
(26) Johnson, K. L.; Kendall, K.; Roberts, A. D. *Proc. R. Soc. London A* **1971**, *324*, 301.
(27) Merrill, W. W.; Pocius, A. V.; Thakkar, B. V.; Tirrell, M. *Langmuir* **1991**, *7*, 1975.
(28) Kurata, M.; Tsunashima, Y. Viscosity-Molecular Weight Relationships and Unperturbed Dimensions of Linear Chain Molecules. In *Polymer Handbook*, 3rd Ed.; Brandrup, J., Immergut, E. H., Eds.; John Wiley and Sons: New York, 1989; Section VII.
(29) Flory, P. J. *Principles of Polymer Chemistry*; Cornell University Press: Ithaca, NY, 1953.
(30) It is well-known that the exponent ν estimated from $[\eta] \sim \langle s^2 \rangle / M$ is somewhat smaller than that directly determined for $\langle s^2 \rangle$. However, the ratio of $\langle s^2 \rangle$ of PI and PS having the same M would be estimated by eq 3 with negligible error.
(31) Higo, Y.; Ueno, N.; Noda, I. *Polym. J.* **1983**, *15*, 367.
(32) Noda, I.; Kato, N.; Kitano, T.; Nagasawa, M. *Macromolecules* **1981**, *14*, 668.
(33) Noda, I.; Higo, Y.; Ueno, N.; Fujimoto, T. *Macromolecules* **1984**, *17*, 1055.
(34) de Gennes, P.-G. *Scaling Concepts in Polymer Physics*; Cornell University Press: Ithaca, NY, 1979.
(35) Leibler, L. *Makromol. Chem., Macromol. Symp.* **1988**, *16*, 1. Witten, T. A.; Leibler, L.; Pincus, P. *Macromolecules* **1990**, *23*, 824. Joanny, J.-F. *Langmuir* **1992**, *8*, 989. Murat, M.; Grest, G. S. *Phys. Rev. Lett.* **1989**, *63*, 1074; *Macromolecules* **1989**, *22*, 4054; *Macromolecules* **1991**, *24*, 704. Klein, J.; Perahia, D.; Warburg, S. *Nature 352*, 143.
(36) Milner, S. T. *Europhys. Lett.* **1988**, *7*, 695. Taunton, H. J.; Toprakcioglu, C.; Fetters, L. J.; Klein, J. *Macromolecules* **1990**, *23*, 571.
(37) Zhulina, E. B.; Borisov, O. V.; Pryamitsin, V. A. *Vysokomol. Soedin.* **1989**, *31A*, 185; *J. Colloid Interface Sci.* **1990**, *137*, 495.
(38) Shim, D. F. K.; Cates, M. E. *J. Phys. (Paris)* **1990**, *51*, 701.
(39) Wu, S. Surface and Interfacial Tensions of Polymers, Plasticizers and Organic Pigments, In *Polymer Handbook*, 3rd ed.; Brandrup, J., Immergut, E. H., Eds.; John Wiley and Sons: New York, 1989; Section VI.
(40) Parsonage, E. E.; Watanabe, H.; Dhoot, S.; Tirrell, M. *Polym. J. (Tokyo)* **1991**, *23*, 641.
(41) Watanabe, H.; Patel, S. S.; Argillier, J.-F.; Parsonage, E. E.; Mays, J. M.; Dan, N.; Tirrell, M. *Mater. Res. Soc. Symp. Proc.* **1992**, *249*, 255.